J Therm Anal Calorim (2012) 107:733–743
DOI 10.1007/s10973-011-1637-z

Combined effect of β-nucleating agent and multi-walled carbon nanotubes on polymorphic composition and morphology of isotactic polypropylene

Nan Zhang · Qin Zhang · Ke Wang · Hua Deng · Qiang Fu

Received: 24 January 2011 / Accepted: 4 May 2011 / Published online: 18 May 2011

Abstract The effects of nucleating duality, imposed by a mixed nucleating agent (NA) system containing multi-walled carbon nanotubes (MWCNTs) and a rare earth (WBG), on the crystallization behaviors of isotactic polypropylene (iPP) including the peak temperature of crystallization (T_{cp}), polymorphic composition, and crystalline morphology, were probed in detail by calorimetry, X-ray diffraction, and polarized light microscopy. In such mixed nucleating agent system, MWCNTs is active filler to induce α-nucleation for iPP, while WBG serves as β-nucleating agent. When the WBG content was low (0.05%), the crystals of WBG were as a form of individual isotropic dendrite, and the enhancement of T_{cp} was achieved by the incorporation of MWCNTs. As the WBG content was high as 0.1%, a percolated NA network consisted of needlelike crystals of WBG yielded before nucleating the prevalent crystallization of iPP. In this case, the addition of MWCNTs has no obvious effect on T_{cp}. However, by varying the mass proportion of MWCNTs/WBG, the polymorphic composition was adjusted significantly, indicating a nucleation competition between MWCNTs and WBG. Although the competitive growth existed between α-crystals nucleated by MWCNTs and β-crystals nucleated by WBG, the formation of primary β-crystallite was always prior to the α-nucleated crystallization, as confirmed by crystalline morphology. These findings are useful for developing a new pathway to prepare iPP-based composite with good mechanical property via the addition of mixed nucleating system containing active inorganic filler and β-nucleating agent.

Keywords Carbon nanotubes · β-Nucleating agent · Polymorphic composition · Morphology

N. Zhang · Q. Zhang · K. Wang (✉) · H. Deng · Q. Fu (✉)
College of Polymer Science and Engineering, State Key Laboratory of Polymer Materials Engineering, Sichuan University, Chengdu 610065, People's Republic of China
e-mail: wkestar@scu.edu.cn

Q. Fu
e-mail: qiangfu@scu.edu.cn

Introduction

As one of the most important semicrystalline polymers, isotactic polypropylene (iPP) has been widely studied for its polymorphic characteristic (monoclinic α-modification, trigonal β-modification, orthorhombic γ-modification, and smectic phase) [1–4]. The α-modification is the most stable and commonly observed, and the β-modification is a metastable crystalline phase that is obtained only under special crystallization conditions or by adding selective β-nucleating agent (NA), and the other two modifications are rarely seen, especially for the most common Ziegler–Natta iPP [5]. It is well known that the nature of α-modification is rigid, which is responsible for strength and modulus, and that of β-modification is easily deformable to bring out good ductility and toughness. Logically, the adjustment of polymorphic behavior seems to be important and interesting for realizing the excellent comprehensive mechanics in iPP product. To attain the evident β-modification in iPP, the introduction of β-nucleating agent is the most convenient method. There are mainly four kinds of β-nucleating agent: a minority of aromatic ring compounds [6, 7], certain group IIA metal salts or their mixtures with some specific dicarboxylic acids [8–11], some substituted aromatic bisamides [12–14], and rare earth β-nucleating agents [15–18]. Except for altering the loading and nucleating duality of β-nucleating agent, a variety of

crystallization conditions like the final temperature of heating, thermal conditions during cooling and crystallization, etc., can impact the polymorphic composition and morphology [5, 14, 18]. Moreover, Chen et al. [19] proposed a new pathway to modulate the polymorphic composition of iPP via a competition between shear flow and heterogeneous nucleation of β-nucleating agent.

On the other hand, many types of inorganic fillers like talc [20, 21], mica [22], calcium carbonate [23–27], and organoclay [28] can act as nucleating agent for iPP. Among these inorganic fillers with nucleating capability, the fibrillous type likes glass fiber (GF) and carbon fiber (CF) has attained intense attention, due to their high efficiency of reinforcement for iPP products. There exists a difference between the nucleating efficiencies of GF and CF. A transcrystallization might occur around CF upon quiescent isothermal crystallization condition, indicating strong nucleating ability [29], whereas shearing field should be introduced for yielding the transcrystalline superstructure around GF [30]. Carbon nanotubes (CNTs), as novel fibrillous fillers, have been extraordinarily developed in recent years. Especially, CNTs possess an extraordinary nucleation capability that a relatively low content (less than 1 wt%) may significantly increase the density of the nuclei and crystallization temperature, and decrease the crystal size and crystallization time [31–35]. Thus, a topic is proposed as that: if the competition between inorganic filler and common nucleating agent is an effective pathway to modulate the polymorphic composition and morphology of iPP. Besides, from a viewpoint of performance modification, except for mechanical reinforcement, the incorporation of inorganic filler into iPP may result in other functionalities, such as thermal stability, flame resistance and electronic conductivity. It may be meaningful for achieving iPP-based composite with comprehensive performance and good processability by incorporation of both inorganic filler and nucleating agent. However, only less attention was by far focused on the combined nucleating effect of inorganic filler and common nucleating agent on the crystallization behavior of iPP. Tang et al. [36] studied the crystallization temperature and morphology of iPP containing organic nucleating agent (aliphatic triamine) and zinc oxide nanoparticles. The non-isothermal crystallization temperature of iPP was improved by 7 °C when organic nucleating agent was distributed within polymeric matrix as a manner of coating onto zinc oxide nanoparticles. Huang et al. [27] investigated the non-isothermal crystallization behavior of polypropylene nucleated by nano-calcium carbonate (nm-$CaCO_3$) and dibenzylidene sorbitol (DBS). There was a synergetic effect of DBS and nm-$CaCO_3$ for the crystallization rate, and the peak temperature of crystallization increased with increasing the amount of DBS.

This study deals with a mixed nucleating system consisted of multi-walled carbon nanotubes (MWCNTs) and a rare earth (WBG), which may impose a dual nucleation impact on iPP. For this mixed nucleating system, MWCNTs act as α-nucleating agent to facilitate the formation of α-iPP, whereas the β-modification is arisen from the rare earth nucleating agent of WBG. The rare earth, WBG, is a new kind of β-nucleating agent for iPP with high efficiency and high selectivity, and was first synthesized by Feng's group [16, 17]. It is a dissolution-type nucleating agent can be partially or totally dissolved in the molten polymer matrix, and then self-assemble into different profiles depending on the temperature and loading during the non-isothermal cooling crystallization process. The group has revealed that the crystalline morphology of WBG-nucleated iPP was strongly dependent on the final temperature of heating [18]. Three types of β-crystalline morphologies, β-spherulite, β-transcrystalline entity, and "flower"-like agglomerate of β-crystallites, were observed with the increasing of final temperature of heating. We also found that WBG concentration has great impact on the β-form content, crystalline morphology, and mechanical properties of β-nucleated iPP [37]. In this study, the interplays of MWCNTs and WBG on the peak temperature of the crystallization during cooling (correlated with the heterogeneously nucleating efficiency), polymorphic composition and crystalline morphology of iPP are investigated in detail. Especially, the competition between α-modification growth and β-modification growth, dominated by the variation of mass proportion of inorganic filler/β-nucleating agent, will be demonstrated clearly. The findings of this study are useful for developing a new pathway to prepare iPP-based composite with good mechanical property via the addition of mixed nucleating system containing active inorganic filler and β-nucleating agent.

Experimental section

Materials

A powder iPP with a melt flow index (MFI) of 8.5 g 10 min^{-1} (230 °C, 2.16 kg) was commercially purchased from Baota Petrochemical Ltd. Co. (Ningxia, China). A small amount of antioxidant (Irganox 1010) is used to prevent degradation of iPP. Raw MWCNTs was purchased from Shenzhen Nanotechnology Ltd. Co. The diameter of the raw MWCNTs ranges from 10 to 20 nm and their length was about 5–15 μm, the purity is more than 95%, and ash (catalyst residue) is less than 0.2%. Before compounding, MWCNTs were burned in muffle at 500 °C for 1 h to reduce defects and form some oxygen-containing groups on the surface [38]. The rare earth β-nucleating

agent, marked as WBG-II, was kindly supplied by Winner Functional Materials (Foshan, China). It is a heteronuclear dimetal complex with a general formula of $Ca_xLa_{1-x}(LIG1)_m(LIG2)_n$, while LIG1 and LIG2 are a dicarboxylic acid and amide-type ligand, respectively. x and $1-x$ are the proportion of Ca^{2+} and La^{3+} ion in the complex, respectively, while m and n are coordination numbers for LIG1 and LIG2, respectively [16].

Sample preparation

To achieve a good dispersion of MWCNTs and WBG in iPP, the samples were prepared with a two-step procedure. First, MWCNTs and WBG were blended with iPP powder in a high-speed mixer at room temperature, the vane speed was 25,000 rpm and mixing time was 90 s. Then, the compound was melt blended in a Haake Rhomix internal mixer at 200 °C upon 50 rpm for 10 min. For comparison, the pure iPP, WBG-nucleated iPP, and MWCNTs-filled iPP were also prepared under the same processing procedure. The resultant samples, used for testing and characterization, were named as pure iPP, xWBG (WBG-nucleated iPP), yCNT (MWCNT-filled iPP), and xW/yC (WBG-nucleated, MWCNT-filled iPP), while x (0.05, 0.1%), y (0.1, 0.2, 0.5, 1, 1.5, 2, 3, and 5%) represent the concentration of WBG and MWCNTs, respectively.

Characterizations

Differential scanning calorimetry (DSC)

The non-isothermal crystallization behavior was recorded using a Perkin-Elmer pyris-I DSC instrument with nitrogen as purge gas, calibrated by indium. The mass of the tested sample was about 5 mg. In order to inspect the crystallization behavior of the samples containing various WBG concentrations, each sample was heated to 200 °C and held for 5 min to eliminate any thermal history, and then cooled to 50 °C at a rate of 10 °C min^{-1}.

Wide angle X-ray diffraction (WAXD)

The WAXD tests were carried out on a Philips X'Pert pro MPD instrument. A conventional Cu K_α ($\lambda = 0.154$ nm, reflection mode) X-ray tube at a voltage of 40 kV and a filament current of 40 mA was used to obtain WAXD spectra. Importantly, to obtain a better understanding on the crystallization behaviors, the samples were first melt and hot pressed into thin films on a hot stage (Linkam THMS 600), and then they were kept molten for 5 min to erase any thermal history. After that they were cooled to room temperature at the cooling rate of 10 °C min^{-1}. The WAXD testing was conducted at a 2θ range from 2° to 40° and a scanning rate of 3° min^{-1}. In the iPP diffraction profile (110) at $2\theta = 14.1°$, (040) at 16.9°, and (130) at 18.5° are the principal reflections of the α-crystal form, while (300) at about 15.9° is the principal reflection of the β-crystal form. The overall crystallinity (X_{all}) and relative content of different crystal forms of iPP can be calculated from the following equations [39, 40]:

$$X_{all} = 1 - \frac{A_{amorphous}}{\sum A_{amorphous} + A_{crystallization}} \quad (1)$$

$$K_\beta = \frac{A_{\beta(300)}}{A_{\alpha(110)} + A_{\alpha(040)} + A_{\beta(300)}} \quad (2)$$

$$X_\beta = K_\beta X_{all} \quad (3)$$

where $A_{amorphous}$ and $A_{crystallization}$ are the areas of amorphous and crystalline peaks, respectively; K_β represents the relative content of the β-crystal form with respect to the α-crystal form; $A_{\beta(300)}$ represents the area of the (300) reflection peak; $A_{\alpha(110)}$, $A_{\alpha(040)}$, and $A_{\alpha(130)}$ represent the areas of the (110), (040), and (130) reflection peaks, respectively.

Polarized light microscope (PLM)

Morphological observations of α- and β-crystals growth were performed on a Leica DMIP polarized light microscopy (PLM) equipped with a Linkam THMS 600 hot stage under crossed polarizer. First, a slice with 20 μm thickness was placed between two glass slides and was heated to melt completely; Second, the sample was heated to 200 °C on the hot stage and kept for 5 min to erase the thermal history; Third, the sample was cooled down to the room temperature at a cooling rate of 10 °C min^{-1}. The morphological photographs of crystallization recorded by a digital camera during cooling were enlarged by 200 times.

Results and discussion

Crystallization of iPP and its filled and/or nucleated systems

The non-isothermal crystallization curves of a series of MWCNTs-filled iPP were recorded by DSC (Fig. 1). It is found that the pure iPP has the lowest peak temperature of crystallization (T_{cp}), 387.7 K, due to homogeneous nucleation process and relatively low nucleation rate. By adding 0.1% MWCNTs, the T_{cp} increases significantly to 396.8 K, indicating a high nucleating efficiency of MWCNTs for iPP. But further increasing the MWCNTs, the increment of T_{cp} becomes slowly, from 396.8 to 399 K within a range from 0.1 to 2%, and unexpectedly the T_{cp} of 0.2%

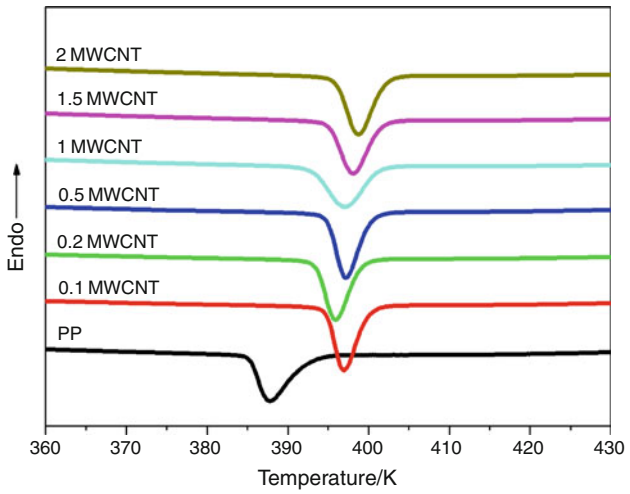

Fig. 1 The non-isothermal crystallization curves of a series of MWCNTs-filled iPP

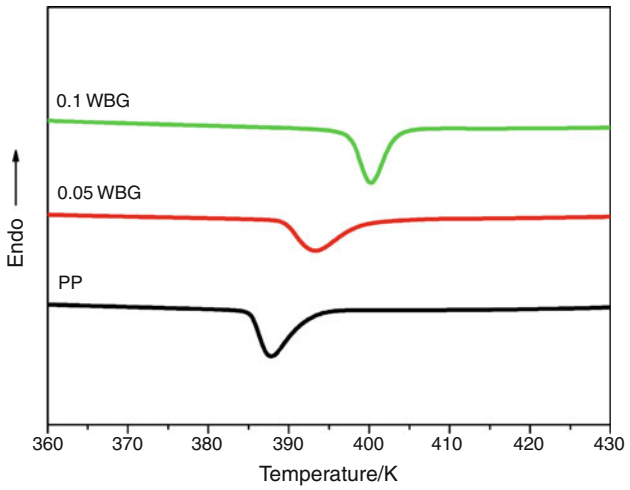

Fig. 2 The non-isothermal crystallization curves of WBG-nucleated iPP

(385.8 K) is even lower than that of 0.1%. The slowly increased trend and the unexpectedly decreased T_{cp} at 0.2% MWCNTs might be attributed to the relatively bad dispersion of MWCNTs at the higher MWCNTs contents, as compared to the 0.1% content. The non-isothermal crystallization curves of WBG-nucleated iPP are illustrated in Fig. 2. For the WBG-nucleated iPP, the heterogeneous nucleation effect is strongly dependent on the WBG content. The introduction of 0.1% WBG results in a significantly increased T_{cp} (400.2 K), which is much higher than that induced by 0.05% WBG (393.4 K). On the other hand, by comparing the T_{cp}s at a same nucleating agent content, i.e., 0.1%, it can be concluded that the nucleating efficiency of WBG is higher than that of MWCNTs evidently.

Figure 3 shows the WXRD profile of iPP and its filled and β-nucleated systems. The overall crystallinity (X_{all}),

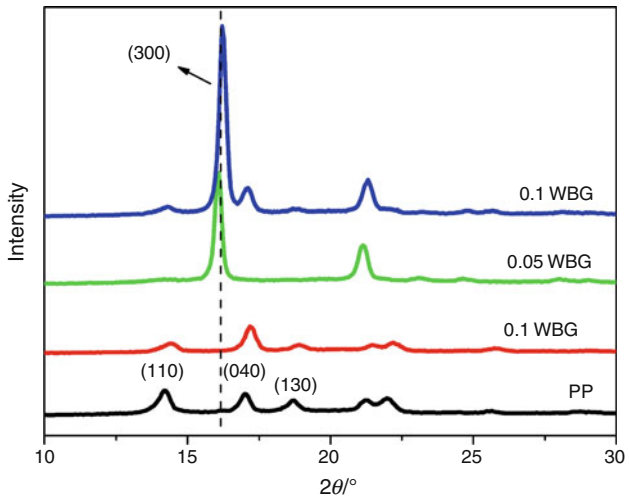

Fig. 3 WXRD profile of iPP and its filled and β-nucleated systems

Table 1 X_{all}, K_β, and K_β results of samples with individual filler or nucleating agent

Sample	X_{all}	K_β	X_β
PP	62.7	\	\
0.1MWCNT	61.6	\	\
0.05WBG	57.9	93.6	54.2
0.1WBG	68.5	76.8	52.6

relative content of β-modification (K_β), and β-crystallinity (X_β) were calculated by Eqs. 1–3 from the WXRD spectra, and the results are listed in Table 1. For the pure iPP and MWCNTs-filled iPP, their overall crystallinities are almost identical and only the α-modification is found. MWCNTs act as α-nucleating agent for iPP. Meanwhile, even by adding a little amount of WBG (0.05%), the crystal form is changed strongly and the K_β reaches as high as 93.6%. It confirms that WBG is a highly selective β-nucleating agent. However, the K_β of 0.1% WBG is much lower than that of 0.05% WBG, only 76.8%. At the same time, the X_{all} of 0.1% WBG is larger for 10% than that of 0.05% WBG, while the X_β of the former is comparable to that of the latter. The β-nucleating efficiency seems to be depressed and the α-modification can be partially nucleated by WBG at the high content, 0.1%. It might be due to the formation of certain supermolecular structure of WBG upon relatively high content, which offers an added α-nucleating ability, namely, the so-called nucleating duality, as similar to other prevalent β-NA likes NU 100 [14]. This explanation will be validated by further polymorphic analysis and crystalline morphology observation in the following section.

The growth processes of crystals of iPP containing MWCNT or nucleating agent were recorded by PLM. The

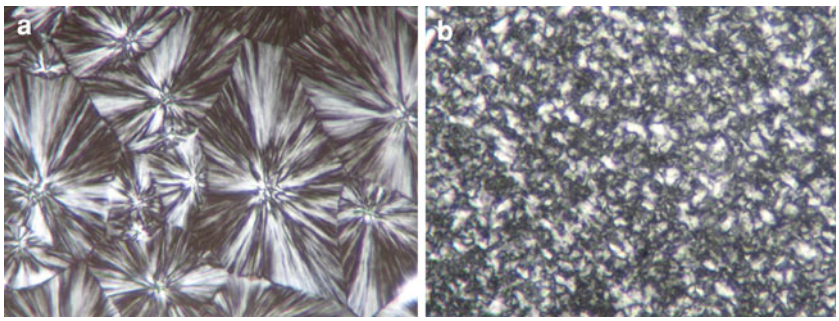

Fig. 4 Final morphologies of **a** pure iPP and **b** 0.1MWCNT

final temperature of heating in PLM experiment is selected as 200 °C. The differences between α-modification and β-modification can be easily distinguished by the observation of PLM. IN general, the β-modification shows highly birefringent (high-light optical) character comparing with the α-modification and will be completely molten at about 155 °C [2]. The final morphologies of the pure iPP and 0.1% MWCNTs are presented in Fig. 4. In these two samples, only α-form spherulites are found, which is well according with the results of WAXD. The crystal size of the former is very big for homogenous nucleation, whereas the crystal size of the later one is much smaller because of strong heterogeneous nucleation and high density of the nuclei. Figure 5 clearly illustrates the crystallization processes of 0.05% WBG (a–c) and 0.1% WBG (d–f), including photographs acquired at the early, intermediate and final stages of crystallization. Different supermolecular structures of β-nucleating agent (WBG) can be recognized. At a low content of 0.05%, WBG substance self-assembles into individual, isotropic dendrites before nucleating β-iPP. Since the crystals of WBG are apart from each other, the subsequent growth of β-crystal follows a spherulite-like manner, which proceeds continuously until the impingement between β-spherulites. At a high content of 0.1%, a majority of WBG substance self-assembles into a highly anisotropic, needlelike superstructure. It should be noted that these needlelike entities could connect with each other to establish a percolated NA network. This physical behavior is also found for the fibrillar α-nucleating agent, MDBS [41]. Therefore, the nucleated crystallization of iPP is based on a framework composed by these needlelike primary crystallites of WBG.

Crystallization properties of iPP with compounded nucleating agent system

To elucidate the compounded influence of MWCNTs and WBG on the crystallization behaviors of iPP, two series of samples with a fixed WBG content as 0.05 or 0.1% and the variable MWCNTs content (0.1–5%) are investigated comparatively. The non-isothermal crystallization curves of WBG-nucleated iPP filled with MWCNTs (*x*W/*y*C sample) are shown in Fig. 6. Especially, the corresponding T_{cp}s are plotted as a function of MWCNTs content in Fig. 7. For the 0.05W/*y*C samples, the T_{cp} increases with the MWCNTs content continuously until 1.5% content. The incorporation of 0.1% MWCNTs results in an obvious increment of 3 K in T_{cp} (from 393.4 to 396.2 K), while the increased trend becomes slow within the content range from 0.1 to 1.5% (from 396.2 to 399.3 K). Although the T_{cp}s of 0.05W/*y*C are higher than that of 0.05WBG, it cannot be concluded that a synergetic nucleation effect exists to accelerate the crystallization of iPP. The T_{cp} versus MWCNTs content curve of the 0.05W/*y*C is similar to that for the MWCNTs-filled samples, and these two

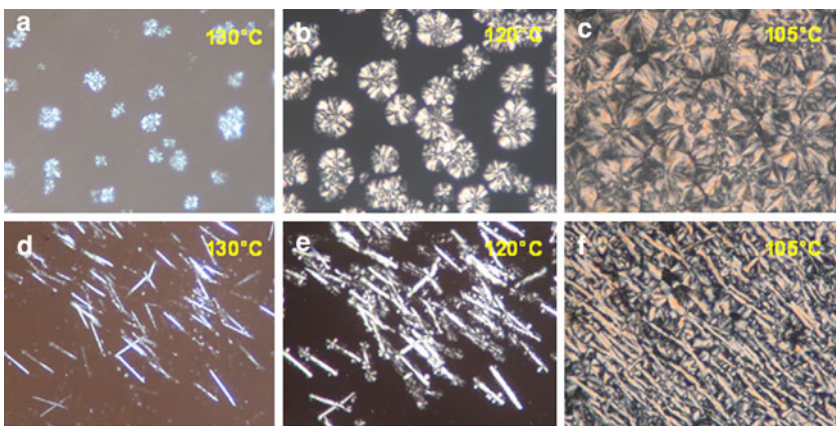

Fig. 5 Crystallization processes of 0.05WBG (**a**–**c**) and 0.1WBG (**d**–**f**), including the early, intermediate, and final stages

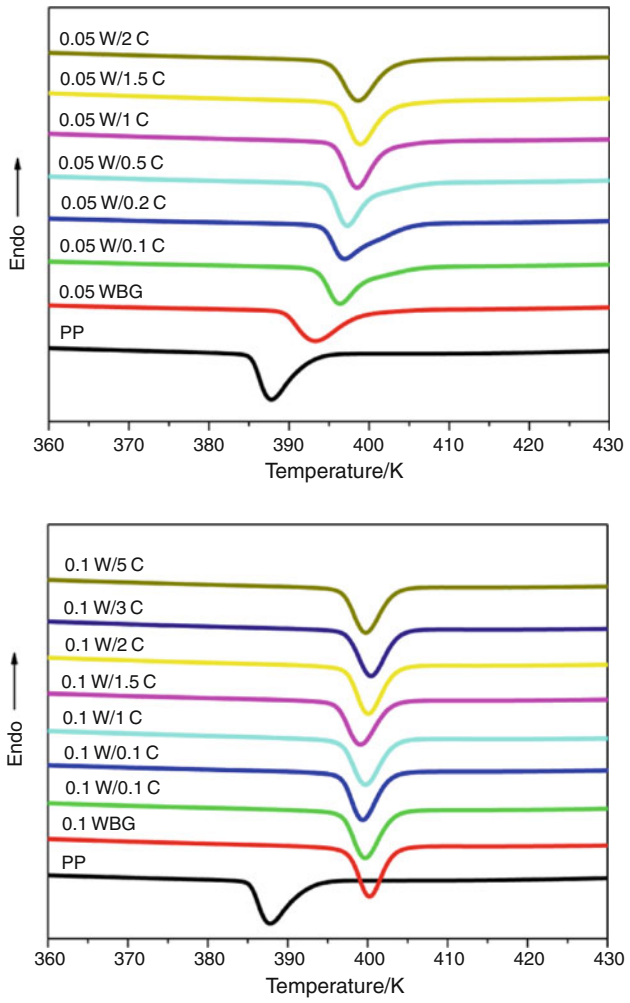

Fig. 6 The non-isothermal crystallization curves of WBG-nucleated iPP filled with MWCNTs

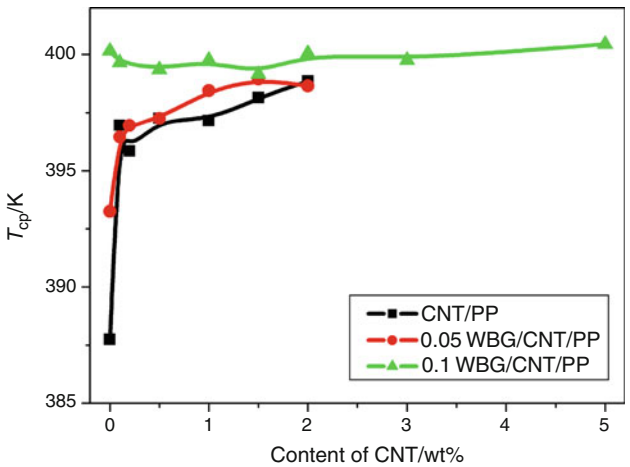

Fig. 7 The crystallization peak temperature (T_{cp}) of MWCNTs-filled iPP with or without WBG

curves almost superpose together, indicating that MWCNTs mainly affects the T_{cp} when the WBG content is low as 0.05%. As to the 0.1W/*y*C samples, the T_{cp} varies

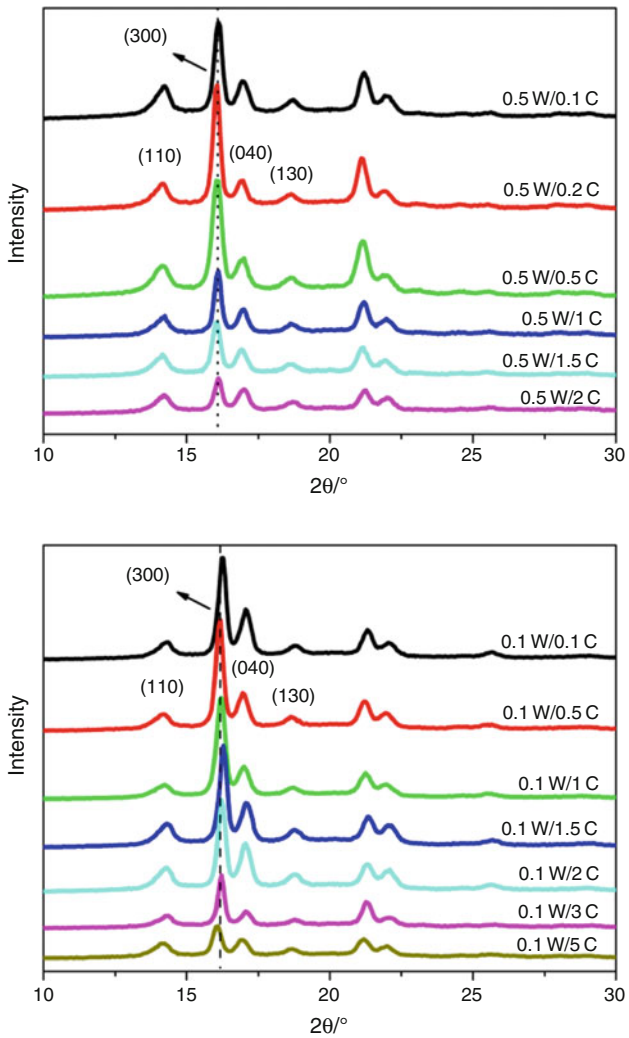

Fig. 8 WXRD profiles of iPP with the compounded NA system

within a narrow temperature range (399.3–400.4 K) for the whole MWCNTs contents range from 0 to 5%. This implies that the T_{cp} is independent on the MWCNTs content, and it is mainly dominated by WBG. Therefore, for both 0.05W/*y*C and 0.1W/*y*C samples, the heterogeneously nucleated crystallization rate is controlled by the NA component whose nucleation efficiency is higher. It is difficult to induce a synergetic nucleation effect to accelerate the iPP crystallization remarkably by adding two kinds of high-effective NAs.

However, the polymorphic behavior of *x*W/*y*C sample can be adjusted prominently by varying the mass proportion of MWCNTs/β-nucleating agent. The WXRD profiles of iPP with the compounded NA system are shown in Fig. 8. The overall crystallinity (X_{all}), relative content of β-modification (K_β), and β-crystallinity (X_β) of iPP with the compounded NA system are listed in Table 2. Meanwhile, K_β and X_{all} as a function of the absolute and/or relative MWCNTs content in the compounded nucleating

Table 2 X_{all}, K_β, and X_β results of samples with the compounded NA system

Sample	X_{all}	K_β	X_β
0.05W/0.1C	64.6	44.8	28.9
0.05W/0.2C	59.0	56.6	33.4
0.05W/0.5C	60.6	54.2	32.8
0.05W/1C	56.5	44.4	25.1
0.05W/1.5C	56.0	41.0	22.9
0.05W/2C	54.8	30.1	16.5
0.1W/0.1C	68.8	49.4	33.9
0.1W/0.5C	68.7	55.3	37.9
0.1W/1C	67.9	61.4	41.6
0.1W/1.5C	62.6	47.4	29.6
0.1W/2C	64.3	43.6	28.0
0.1W/3C	59.6	49.1	29.3
0.1W/5C	57.5	36.2	20.8

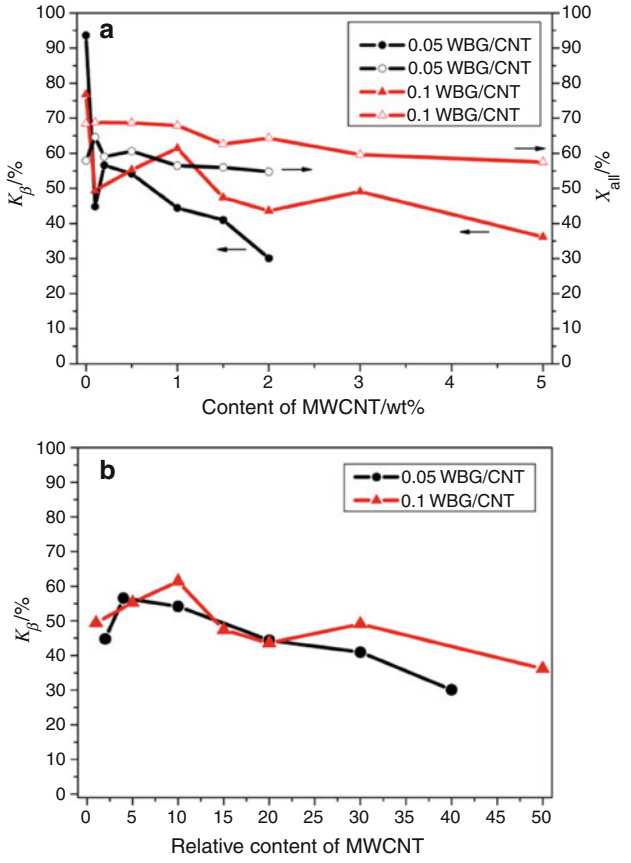

Fig. 9 **a** K_β and X_{all} as a function of the absolute MWCNTs content in the compounded nucleating system; **b** K_β as a function of the relative MWCNTs content in the compounded nucleating system

system are illustrated in Fig. 9a and b, respectively. For both of 0.05W/*y*C and 0.1W/*y*C samples, it can be roughly concluded that the X_{all} is decreased for 10% as the MWCNTs content increased. Whereas the K_β dependence on the MWCNTs content is somewhat complicated. Comparing with samples including individual β-NA, the β-crystal content is strongly depressed by incorporation of MWCNTs because of its pronounced α-nucleating ability. However, K_β increases first with MWCNTs content increase, and there is a highest K_β at certain MWCNTs content. Then K_β decreases continuously when further increase MWCNTs content. The highest K_β is 56.6% at 0.2% MWCNTs content for 0.05W/*y*C, while it is 61.4% at 1% MWCNTs content for 0.1W/*y*C. Meanwhile, the highest K_β is approximately two times for that of the lowest one, indicating an effective adjustment of polymorphic composition by the variation of MWCNTs/WBG proportion. Correspondingly, the change of X_β as a function of MWCNTs content is the same as that of K_β for both kinds of sample. Obviously the introduction of both high-efficient β-NA and active filler with good α-nucleating ability into iPP may induce a competitive growth between α-modification and β-modification. By altering the nucleating ability of α-NA component or β-NA component, the formation of certain crystalline modification is depressed or promoted, resulting in a significant change in the polymorphic behavior. As a routine consideration, the β-nucleating ability of WBG should be depressed more and more with the increasing of α-NA (MWCNTs) content. The exact mechanism of the abnormal increment of K_β at the early stage of increasing MWCNTs content is not yet completely clear. Logically, it might be arisen from the interplay of the following two issues: (1) the dispersion state of MWCNTs; (2) the dissolvability and self-assembled supermolecular structure of WBG substance. The dissolvability and self-assembled supermolecular structure of NA substance can be impacted strongly by the final temperature of heating, NA content, cooling rate, isothermal crystallization temperature, etc., which have been validated on many α- and/or β-nucleating agents, such as sorbitol derivatives [41–43], aromatic phosphorus salts [44], aryl amide derivative [45, 46], and aromatic bisamide [13, 14]. Therefore, the incorporation of MWCNTs can also affect the formation of supermolecular structure of WBG crystals formed during cooling, especially disturb the WBG network yielded at high WBG content, which will be confirmed by the crystalline morphology observation subsequently.

The evolution of polymorphic morphology of the 0.05W/0.1C sample is shown in Fig. 10. The isotropic WBG-dendrites generate first, and then they direct the formation of β-spherulite. Unlike the 0.05 WBG sample that is occupied by β-spherulite totally, the α-modification region appears at the latter stage of crystallization. Meanwhile the β-spherulites are surrounded by the α-modification region. To distinct the α- and β-crystalline regions clearly, the selectively melt experiment at 155 °C has been

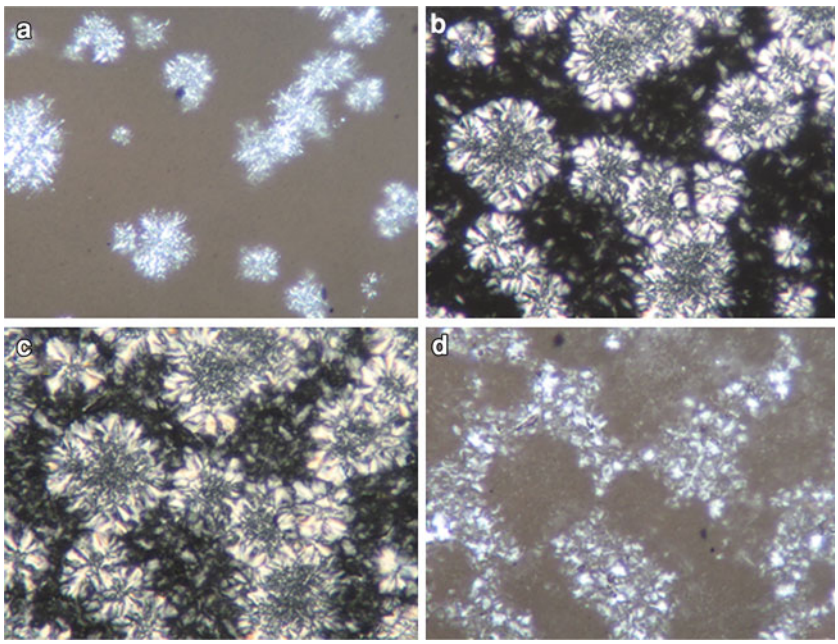

Fig. 10 Crystallization processes of **a–c** 0.05W/0.1C and **d** the α-phase structures left behind after the separate melting of the β-phase at 155 °C

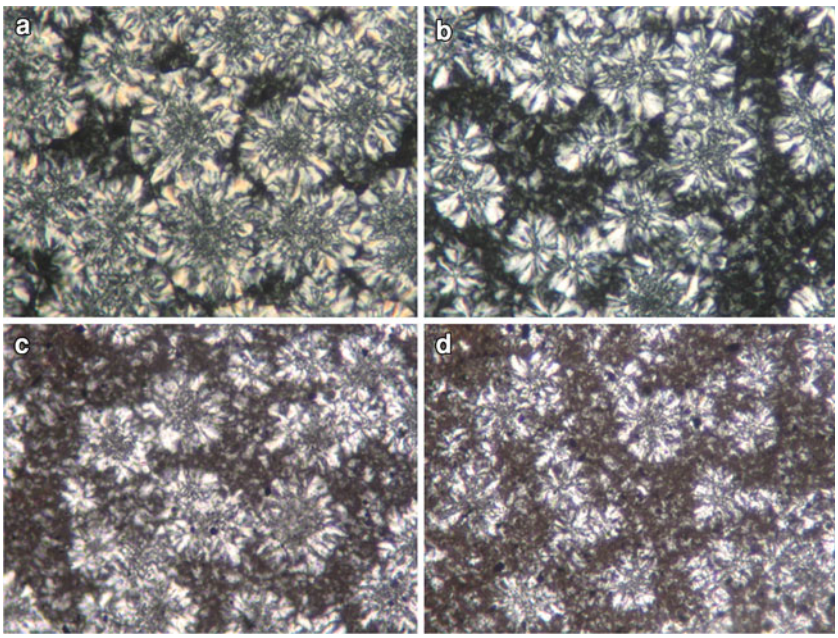

Fig. 11 Morphologies of 0.05wt% WBG-nucleated iPP with various MWCNT contents **a** 0.05W/0.2C, **b** 0.05W/0.5C, **c** 0.05W/1C, and **d** 0.05W/2C

done, and the result is presented as Fig. 10d. The early formed, high-light spherulite domains are molten at 155 °C, while the later formed circle crystalline region is preserved, confirming they are β- and α-modification, respectively. The polymorphic morphologies at higher MWCNTs contents (0.2–2%) are presented in Fig. 11. In general, these crystalline morphologies are identical with the 0.05W/0.1C sample. Moreover, it should be noted that the area fraction of highlighted β-modification region is highest at the MWCNTs content of 0.2%, which is well agreed with the polymorphic composition analysis.

The evolution of polymorphic morphology of the 0.1W/0.1C sample is shown in Fig. 12. As to the 0.1% WBG content, the crystalline growth fashion of the 0.1W/0.1C sample is similar to that of the 0.1WBG sample as that: the needlelike crystals of WBG first appear, which constitute the percolated β-NA network; the further crystallization proceeds on the framework consisted of needlelike WBG crystals, namely, the PP crystalline growth around and/or between these needlelike entities. After experiencing the selective melting, as shown in Fig. 12d, the residual crystalline morphology significantly differs from that of

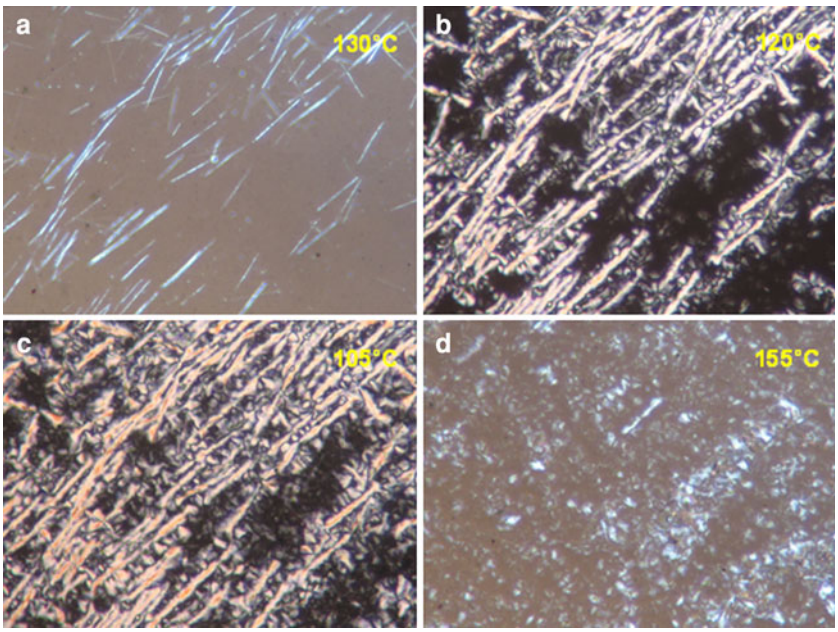

Fig. 12 Crystallization processes of **a–c** 0.1W/0.1C and **d** the α-phase structures left behind after the separate melting of the β-phase at 155 °C

0.05W/0.1C. The survived α-crystals exist everywhere, and no α-dominant or β-dominant region is found. Two conclusions can be deduced from this phenomenon as that: (1) the β-NA network results in the α- and β-crystalline regions penetrate into each other, (2) the needlelike supermolecular structure of WBG substance possesses the nucleating duality that can nucleate both of α- and β-modification. The polymorphic morphologies at higher MWCNTs contents (1–5%) are presented in Fig. 13. The formation of needlelike supermolecular structure of WBG seems to be depressed by adding more amounts of MWCNTs. Although the needlelike crystals of WBG can also generate at the MWCNTs contents of 1 and 2%, the connection between the needlelike entities is weakened, even the individual, anisotropic highlighted crystals appear at the 2% content. For the higher MWCNTs contents, 3 and 5%, the polymorphic morphology is similar to that of the 0.05W/*y*C samples (Fig. 11). Only the isotropic β-dendrites are found, and the area fraction of highlighted crystal region is reduced evidently at the highest MWCNTs content of 5%.

By comparing the polymorphic morphology between two series of samples, 0.05W/*y*C and 0.1W/*y*C, some conclusions can be drawn. Since the nucleating efficiency

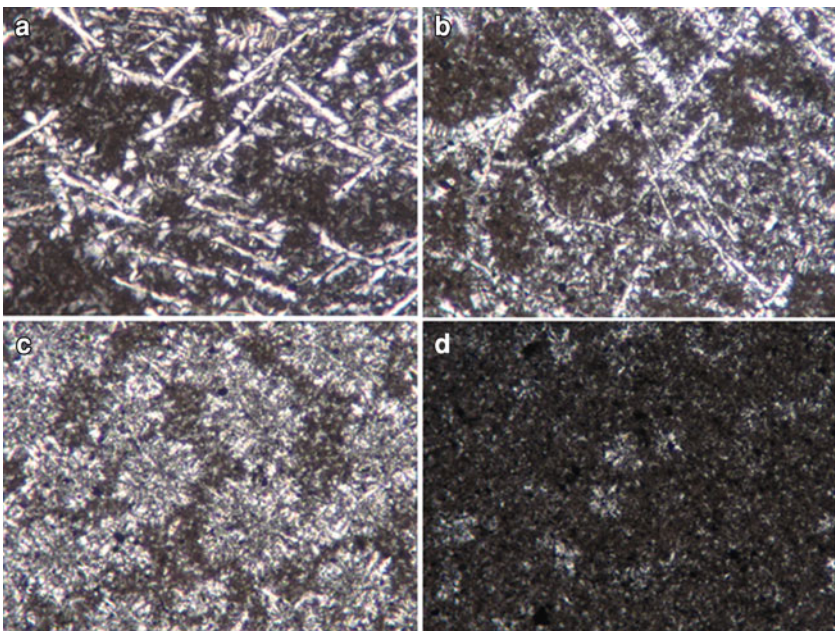

Fig. 13 Morphologies of 0.1wt% WBG-nucleated iPP with various MWCNT contents **a** 0.1W/1C, **b** 0.1W/2C, **c** 0.1W/3C, and **d** 0.1W/5C

of WBG is somewhat higher than that of MWCNTs, the appearance of primary β-crystallite is always prior to the α-nucleated crystallization for whatever sample. For the 0.05W/*y*C samples, the impact of adding MWCNTs on the self-assembled behavior of WBG is weak. Whereas, as the WBG content is high as 0.1%, the incorporation of MWCNTs may depress the formation of needlelike supermolecular structure of WBG substance and disturb the connectivity of the β-NA network.

Conclusions

The compounded nucleating system containing MWCNTs and rare earth WBG can impose a dual nucleating effect on the crystallization of iPP, which may induce a competitive growth between α-crystals nucleated by MWCNTs and β-crystals nucleated by WBG. A synergetic nucleating effect is difficult to be obtained though MWCNTs and WBG are high-efficiency NAs for iPP. However, the polymorphic composition can be adjusted prominently by the variation of filler/β-NA mass proportion. Interestingly, the β-nucleating ability of WBG does not decrease monotonously with the increasing of MWCNTs content. There exists an optimum mass proportion between MWCNTs and WBG to attain the highest K_β. The crystalline morphology observation confirms that: (1) the formation of primary β-crystallite is always prior to the α-nucleated crystallization; (2) the addition of MWCNTs can strongly impact the formation of supermolecular structure of WBG substance and β-NA network, especially at a high WBG content.

Acknowledgements The authors would like to express their sincere thanks to the National Natural Science Foundation of China for Financial Support (21034005, 50903048).

References

1. Lotz B, Wittmann JC, Lovinger AJ. Structure and morphology of poly(propylenes): a molecular analysis. Polymer. 1996;37:4979–92.
2. Varga J. beta-modification of isotactic polypropylene: preparation, structure, processing, properties, and application. J Macromol Sci Phys. 2002;B41:1121–71.
3. Meille SV, Bruckner S, Porzio W. γ-Isotactic polypropylene. A structure with nonparallel chain axes. Macromolecules. 1990;23:4114–21.
4. Brückner S, Meille SV, Petraccone V, Pirozzi B. Polymorphism in isotactic polypropylene. Prog Polym Sci. 1991;16:361–404.
5. Krache R, Benavente R, Lopez-Majada JM, Perena JM, Cerrada ML, Perez E. Competition between alpha, beta, and gamma polymorphs in beta-nucleated metallocenic isotactic polypropylene. Macromolecules. 2007;40:6871–8.
6. Fujiyama M. Structures and properties of injection moldings of beta-crystal nucleator-added polypropylenes. 1. effect of beta-crystal nucleator content. Int Polym Process. 1995;10:172–8.
7. Menyhard A, Varga J, Molnar G. Comparison of different beta-nucleators for isotactic polypropylene, characterisation by DSC and temperature-modulated DSC (TMDSC) measurements. J Therm Anal Calorim. 2006;83:625–30.
8. Varga J, Mudra I, Ehrenstein GW. Highly active thermally stable beta-nucleating agents for isotactic polypropylene. J Appl Polym Sci. 1999;74:2357–68.
9. Dou Q. Effect of metallic salts of pimelic acid and crystallization temperatures on the formation of beta crystalline form in isotactic poly(propylene). J Macromol Sci B Phys. 2007;46:1063–80.
10. Li JX, Cheung WL. Conversion of growth and recrystallisation of beta-phase in doped iPP. Polymer. 1999;40:2085–8.
11. Li JX, Cheung WL, Chan CM. On deformation mechanisms of beta-polypropylene 2. Changes of lamellar structure caused by tensile load. Polymer. 1999;40:2089–102.
12. Kotek J, Raab M, Baldrian J, Grellmann W. The effect of specific beta-nucleation on morphology and mechanical behavior of isotactic polypropylene. J Appl Polym Sci. 2002;85:1174–84.
13. Mohmeyer N, Schmidt HW, Kristiansen PM, Altstadt V. Influence of chemical structure and solubility of bisamide additives on the nucleation of isotactic polypropylene and the improvement of its charge storage properties. Macromolecules. 2006;39:5760–7.
14. Varga J, Menyhard A. Effect of solubility and nucleating duality of *N*, *N*′-dicyclohexyl-2, 6-naphthalenedicarboxamide on the supermolecular structure of isotactic polypropylene. Macromolecules. 2007;40:2422–31.
15. Feng JC, Chen MC. Effects of La3+-containing additive on crystalline characteristics of isotactic polypropylene. Polym Int. 2003;52:42–5.
16. Xiao WC, Wu PY, Feng JC. Effect of beta-nucleating agents on crystallization and melting behavior of isotactic polypropylene. J Appl Polym Sci. 2008;108:3370–9.
17. Xiao WC, Wu PY, Feng JC, Yao RY. Influence of a novel beta-nucleating agent on the structure, morphology, and nonisothermal crystallization behavior of isotactic polypropylene. J Appl Polym Sci. 2009;111:1076–85.
18. Luo F, Geng CZ, Wang K, Deng H, Chen F, Fu Q, Na B. New understanding in tuning toughness of beta-polypropylene: the role of beta-nucleated crystalline morphology. Macromolecules. 2009;42:9325–31.
19. Chen YH, Mao YM, Li ZM, Hsiao BS. Competitive growth of alpha- and beta-crystals in beta-nucleated isotactic polypropylene under shear flow. Macromolecules. 2010;43:6760–71.
20. Varga J, Tóth FS. Filled compounds of the beta-modification of polypropylene. Die Angew Makromol Chem. 1991;188:11–25.
21. Tjong SC, Li RKY. Mechanical properties and impact toughness of talc-filled beta-crystalline phase polypropylene composites. J Vinyl Addit Technol. 1997;3:89–95.
22. Fujiyama M. Structure and properties of injection moldings of beta-crystal nucleator-added PP—Part 6, addition of beta-crystal nucleator to particulate-filled polypropylenes. Int Polym Process. 1998;13:411–6.
23. Tjong SC, Xu SA. Non-isothermal crystallization kinetics of calcium carbonate filled beta-crystalline phase polypropylene composites. Polym Int. 1997;44:95–103.
24. Labour T, Gauthier C, Seguela R, Vigier G, Bomal Y, Orange G. Influence of the beta crystalline phase on the mechanical properties of unfilled and $CaCO_3$-filled polypropylene. I. Structural and mechanical characterisation. Polymer. 2001;42:7127–35.
25. Labour T, Vigier G, Seguela R, Gauthier C, Orange G, Bomal Y. Influence of the beta-crystalline phase on the mechanical properties of unfilled and calcium carbonate-filled polypropylene: ductile cracking and impact behavior. J Polym Sci B Polym Phys. 2002;40:31–42.

26. Kotek J, Kelnar I, Baldrian J, Raab M. Tensile behaviour of isotactic polypropylene modified by specific nucleation and active fillers. Eur Polym J. 2004;40:679–84.
27. Huang YP, Chen GM, Yao Z, Li HW, Wu Y. Non-isothermal crystallization behavior of polypropylene with nucleating agents and nano-calcium carbonate. Eur Polym J. 2005;41:2753–60.
28. Ghugare SV, Govindaiah P, Avadhani CV. Polypropylene-organoclay nanocomposites containing nucleating agents. Polym Bull. 2009;63:897–909.
29. Varga J, Karger-Kocsis J. Interfacial morphologies in carbon fibre-reinforced polypropylene composites. Polymer. 1995;36:4877–81.
30. Varga J, Karger-Kocsis J. The occurance of transcrystallization or row-nucleated cylindritic crystallization as a result of shearing in a glass-fiber-reinforced polypropylene. Compos Sci Technol. 1993;48:191–8.
31. Valentini L, Biagiotti J, Kenny JM, Santucci S. Effects of single-walled carbon nanotubes on the crystallization behavior of polypropylene. J Appl Polym Sci. 2003;87:708–13.
32. Seo MK, Lee JR, Park SJ. Crystallization kinetics and interfacial behaviors of polypropylene composites reinforced with multi-walled carbon nanotubes. Mater Sci Eng A Struct Mater Prop Microstruct Process. 2005;404:79–84.
33. Assouline E, Lustiger A, Barber AH, Cooper CA, Klein E, Wachtel E, Wagner HD. Nucleation ability of multiwall carbon nanotubes in polypropylene composites. J Polym Sci B Polym Phys. 2003;41:520–7.
34. Grady BP, Pompeo F, Shambaugh RL, Resasco DE. Nucleation of polypropylene crystallization by single-walled carbon nanotubes. J Phys Chem B. 2002;106:5852–8.
35. Lozano K, Barrera EV. Nanofiber-reinforced thermoplastic composites. I. Thermoanalytical and mechanical analyses. J Appl Polym Sci. 2001;79:125–33.
36. Tang JG, Wang Y, Liu HY, Belfiore LA. Effects of organic nucleating agents and zinc oxide nanoparticles on isotactic polypropylene crystallization. Polymer. 2004;45:2081–91.
37. Luo F, Wang K, Ning N, Geng C, Deng H, Chen F, Fu Q, Qian Y, Zheng D. Dependence of mechanical properties on β-form content and crystalline morphology for β-nucleated isotactic polypropylene. Polym Adv Technol. 2011. doi:10.1002/pat.1718.
38. Lee SH, Cho E, Jeon SH, Youn JR. Rheological and electrical properties of polypropylene composites containing functionalized multi-walled carbon nanotubes and compatibilizers. Carbon. 2007;45:2810–22.
39. Huo H, Jiang SC, An LJ, Feng JC. Influence of shear on crystallization behavior of the beta phase in isotactic polypropylene with beta-nucleating agent. Macromolecules. 2004;37:2478–83.
40. Su ZQ, Dong M, Guo ZX, Yu J. Study of polystyrene and acrylomtrile—styrene copolymer as special beta-nucleating agents to induce the crystallization of isotactic polypropylene. Macromolecules. 2007;40:4217–24.
41. Shepard TA, Delsorbo CR, Louth RM, Walborn JL, Norman DA, Harvey NG, Spontak RJ. Self-organization and polyolefin nucleation efficacy of 1, 3:2, 4-di-p-methylbenzylidene sorbitol. J Polym Sci B Polym Phys. 1997;35:2617–28.
42. Kristiansen M, Werner M, Tervoort T, Smith P, Blomenhofer M, Schmidt HW. The binary system isotactic polypropylene/bis (3, 4-dimethylbenzylidene) sorbitol: phase behavior, nucleation, and optical properties. Macromolecules. 2003;36:5150–6.
43. Kobayashi T, Hashimoto T. Development of self-assembling nucleators for highly transparent semi-crystalline polypropylene. Bull Chem Soc Jpn. 2005;78:218–35.
44. Yoshimoto S, Ueda T, Yamanaka K, Kawaguchi A, Tobita E, Haruna T. Epitaxial act of sodium 2, 2′-methylene-bis-(4,6-di-t-butylphenylene) phosphate on isotactic polypropylene. Polymer. 2001;42:9627–31.
45. Dong M, Gu ZX, Yu J, Su ZQ. Crystallization behavior and morphological development of isotactic polypropylene with an aryl amide derivative as beta-form nucleating agent. J Polym Sci B Poly Phys. 2008;46:1725–33.
46. Dong M, Guo ZX, Yu J, Su ZQ. Study of the assembled morphology of aryl amide derivative and its influence on the non-isothermal crystallizations of isotactic polypropylene. J Polym Sci B Polym Phys. 2009;47:314–25.